# Understanding the Primary Synchronization Signals in 3GPP Cellular Networks

Byung-Jae Kwak, Jin Kyeong Kim, Chanho Yoon, Jung Ho Myung, and Young Jo Ko

Mobile Communication Research Division

Electronics and Telecommunications Research Institute

Daejeon, Korea

bjkwak@etri.re.kr, jkkim@etri.re.kr, chyoon@etri.re.kr, jhmyung@etri.re.kr, koyj@etri.re.kr

Abstract—This paper revisits the design of the LTE and 5G NR Primary Synchronization Signals (PSS) and clarifies several misconceptions and answers key questions not easily addressed elsewhere. We show where their characteristic behavior—sharp autocorrelation peaks and low cross-correlations—actually comes from. We also justify frequency-domain mapping over time-domain mapping in OFDM systems. We show that the current 3GPP PSS choices are effective yet not optimal. We also analyze Zadoff-Chu sequences of composite length and demonstrate how specific root selections can produce undesirable cross-correlation peaks, providing guidance for safe root choices. The results offer a unified, implementation-oriented view of existing PSS designs and practical insights for synchronization sequence design in beyond-5G/6G systems.

Index Terms—PSS, synchronization, 3GPP, LTE, 5G NR, beyond-5G/6G, Zadoff-Chu.

#### I. Introduction

The Primary Synchronization Signal (PSS) is a dedicated downlink signal transmitted by a base station to enable user equipment (UE) to achieve initial time and frequency synchronization. Detecting the PSS is the first step a UE takes during cell search, as it provides the timing reference and contributes to cell identity (ID) detection [1].

Given its critical role, the PSS must be carefully designed to enable robust and efficient detection. Desirable characteristics of PSS sequences include a sharp autocorrelation peak, low cross-correlation between different PSS sequences, constant amplitude in the frequency domain, and low peak-to-average power ratio (PAPR) in the time domain. Moreover, PSS sequences should be robust to noise, multipath propagation, and frequency offset [2], [3].

We consider the PSS sequences defined in the 3rd Generation Partnership Project (3GPP) [4] and explore how the desirable characteristics are achieved. Our aim is to clarify often-overlooked aspects that can be confusing for those unfamiliar with the topic. In doing so, we hope to address some fundamental questions that are often left unanswered and

This work was supported by Institute of Information & communications Technology Planning & Evaluation (IITP) grant funded by the Korea government(MSIT) (NO.RS-2024-00397216, Development of Upper-mid band Extreme massive MIMO (E-MIMO) system technology [40%]; NO.RS-2021-II210746, Development of Tbps wireless communication technology [30%]; NO.RS-2024-00444230, Development of Wireless Technology for Integrated Sensing and Communication [30%]).

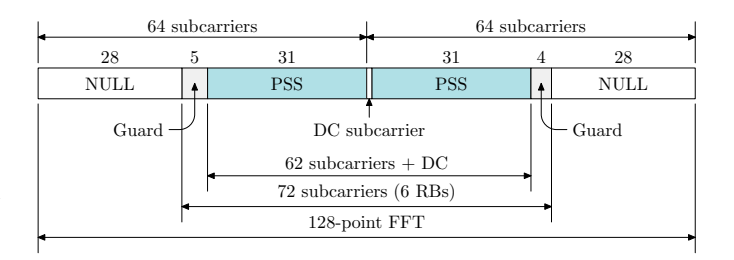


Fig. 1. Frequency-domain structure of the 128-subcarrier window containing the LTE PSS.

clarify common misunderstandings about the PSS sequences in 3GPP.

Our objective is *not* to provide a comprehensive introduction to PSS sequences in 3GPP. We aim to help readers not only understand the current PSSs but also provide insights that will be valuable when designing synchronization sequences for beyond-5G/6G mobile communication systems.

#### II. THE STATE-OF-THE-ART PSS

In 3GPP, Long-Term Evolution (LTE), including its Advanced version (LTE-A), and 5G New Radio (NR) each define their own PSS.

#### A. LTE PSS

In LTE, the PSS is placed at the center of the frequency spectrum, and it spans 62 subcarriers symmetrically centered around the DC subcarrier as illustrated in Fig. 1 [5]. These 62 subcarriers lie within a 72-subcarrier synchronization region, which corresponds to six resource blocks (RBs) in the frequency domain.

The PSS is derived from length-63 Zadoff-Chu sequences defined as:

$$s_u[n] = e^{-j\frac{\pi u n(n+1)}{63}}, \quad 0 \le n < 63,$$
 (1)

where  $u \in \{25, 29, 34\}$  is the root index, identifying one of the three physical-layer cell identity groups  $N_{ID}^{(2)} \in \{0, 1, 2\}$ . The root index u is chosen such that  $\gcd(u, 63) = 1$ , ensuring that the sequence is a *valid* Zadoff-Chu sequence [6]. Only 62 elements of the length-63 sequence are actually mapped onto subcarriers. Since the DC subcarrier is not used, the central element  $s_u[31]$  is omitted.

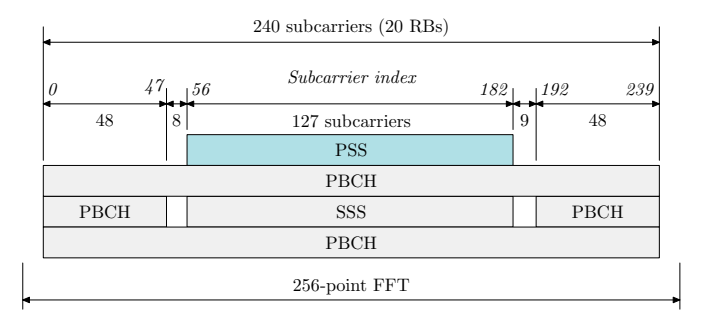


Fig. 2. The structure of 5G NR SSB.

#### B. 5G NR PSS

In 5G NR, the PSS is transmitted as part of a Synchronization Signal Block (SSB), which groups together the PSS, the Secondary Synchronization Signal (SSS), and the Physical Broadcast Channel (PBCH). This grouping supports a structured initial access procedure that is designed to operate with directional transmissions [7].

Fig. 2 illustrates the frequency-domain allocation of the PSS within a 5G NR SSB. The SSB spans 240 subcarriers (equivalent to 20 RBs) inside a 256-point FFT grid. The PSS occupies 127 subcarriers, centered within the 240-subcarrier SSB.

The PSS is constructed using a length-127 m-sequence generated by a linear feedback shift register (LFSR) with the generator polynomial  $x^7 + x^4 + 1$ . The initial state of the LFSR is defined as

$$[s[6], s[5], \dots, s[0]] = [1, 1, 1, 0, 1, 1, 0],$$

which produces the binary sequence s[k]. This sequence is mapped to Binary Phase Shift Keying (BPSK) symbols using the transformation d[k] = 1 - 2s[k]. To support  $N_{ID}^{(2)} \in \{0,1,2\}$ , the PSS sequences are defined by applying cyclic shifts to the base sequence as follows:

$$\begin{aligned} d_0[k] &= 1 - 2s[k] \\ d_1[k] &= 1 - 2s[(k+43) \mod 127] \\ d_2[k] &= 1 - 2s[(k+86) \mod 127] \end{aligned} \tag{2}$$

# III. Frequently Asked Questions & Common Misconceptions

#### A. The Correlation Properties of PSS Sequences

A common misconception is that the correlation properties of LTE and 5G NR PSS sequences are due to the unique properties of Zadoff-Chu sequences and m-sequences. We often see statements like "Zadoff-Chu sequences are used as PSS because they produce a sharp correlation peak". However, those statements are only partially true—in reality, those unique properties play surprisingly minor roles in determining the correlation properties of the PSS sequences.

The inner product of any two valid Zadoff-Chu sequences is  $1/\sqrt{N}$  (approximately zero; nearly orthogonal), where N is the length of the Zadoff-Chu sequences. Zadoff-Chu sequences are also polyphase sequences.

The three LTE PSS sequences are obtained by mapping three length-63 Zadoff-Chu sequences, each generated by a distinct root index, in the frequency domain. Since DFT and IDFT are unitary transforms (with appropriately defined inner product operators), the inner product is preserved between the time and frequency domains [8]. As a result, the corresponding time-domain sequences are also nearly orthogonal—an important property for synchronization. Because Zadoff-Chu sequences are polyphase, power is evenly distributed across the 62 subcarriers, offering robustness in frequency-selective fading channels. Additionally, the polyphase nature of these sequences gives rise to the sharp autocorrelation peaks observed in LTE PSS. (See Section III-B for more details.)

However, being a polyphase sequence is not a unique feature of Zadoff-Chu sequences. Any BPSK- or QPSK-mapped OFDM symbol also qualifies as a polyphase sequence and will exhibit a sharp autocorrelation peak similar to that of the LTE PSS. Moreover, constructing a set of three (strictly) orthogonal sequences is relatively straightforward.

In 5G NR, the three PSS sequences are obtained by applying cyclic shifts to a single m-sequence of length 127. The result is, again, a set of polyphase sequences mapped in the frequency domain, with inner products of exactly 1/N between any pair, making them nearly orthogonal. Other properties of the m-sequence play little role. As in LTE, these characteristics lead to sharp autocorrelation peaks and robustness in frequency-selective fading channels.

The above explanation showed that the correlation properties of 3GPP PSS sequences can be understood without using the special mathematical features of Zadoff-Chu or *m*-sequences. Contrary to common belief, the correlation properties of PSS sequences do not arise from the unique mathematical features of Zadoff-Chu or *m*-sequences. As shown in [9], even random phase sequences can achieve correlation performance comparable to 5G NR PSS. This demonstrates that the observed properties fundamentally stem from general characteristics, such as polyphase structure and the use of frequency-domain mapping, rather than the unique characteristics of Zadoff-Chu or *m*-sequences. These aspects will be discussed in greater detail in the next section.

#### B. Why Frequency Domain Mapping?

As shown in Figs. 1 and 2, the PSS symbols in both LTE and 5G NR are mapped directly onto subcarriers in the *frequency domain*, rather than in the time domain. This may seem surprising, since the Zadoff-Chu sequences and *m*-sequences used for the PSSs in LTE and 5G NR are well known for their desirable correlation properties, and the correlation is performed in the *time domain*. Mapping these sequences directly in the frequency domain, therefore, appears counterintuitive.

So, why frequency domain mapping? Because it solves practical problems while introducing minimal overhead.

 $<sup>^{1}</sup>$ Even though m-sequences are not usually described as polyphase sequences, they are a special case.

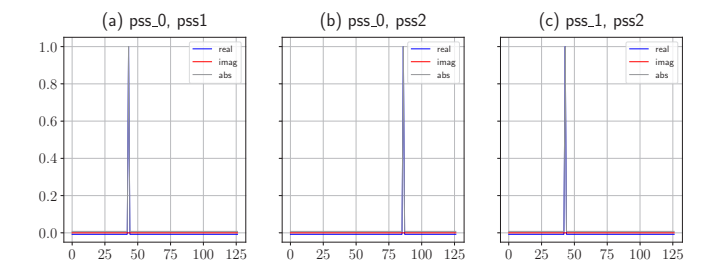


Fig. 3. Periodic cross-correlation of time-domain-mapped 5G NR PSS sequences. Normalized by the length of m-sequence. Peaks at 43, 86, and 43 (i.e., 86-43=43).

# 1) Overhead:

The overhead is minimal because the IFFT is already available as a standard component in OFDM systems.

#### 2) Efficient resource allocation:

Frequency-domain mapping enables efficient resource allocation by allowing precise control over which subcarriers are used, making spectral management easier and avoiding interference with other signals or reserved bands.

#### 3) Guaranteed autocorrelation properties:

Frequency-domain mapping guarantees excellent autocorrelation properties. According to the modulus-one sequence theorem and its corollary (see below), any modulus-one sequence mapped in the frequency domain yields ideal periodic autocorrelation (and consequently excellent aperiodic autocorrelation) characteristics in the time domain [10]. Both Zadoff–Chu sequences and *m*-sequences used in 3GPP PSS are polyphase, and therefore modulus-one sequences. The sharp peaks of autocorrelation do not originate from the unique correlation property of Zadoff–Chu or *m*-sequences, but rather from the fact that they satisfy the modulus-one condition. This represents the most significant benefit of frequency-domain mapping.

#### 4) Improved cross-correlation characteristics:

Frequency-domain mapping significantly improves the time-domain cross-correlation characteristics.

The three sequences in the 5G NR PSS are constructed using cyclic shifts of a single base m-sequence, as defined in (2). Since they are cyclic shifts of one another, if they are used as time-domain sequences, their periodic cross-correlations would produce peaks at shift lags of  $\pm 43$  and  $\pm 86$ , as shown in Fig. 3

These cross-correlation peaks are problematic as they may lead to false detection events during synchronization. Frequency-domain mapping eliminates these artifacts. As shown in Fig. 4, the time-domain periodic cross-correlation peaks are no longer present when the sequences are mapped in the frequency domain.

Unfortunately, Zadoff-Chu sequences are an exception—frequency-domain mapping does not improve their time-domain periodic cross-correlation, leaving spurious peaks that can trigger false detections. See Section III-D for the details.

### 5) Design adaptability:

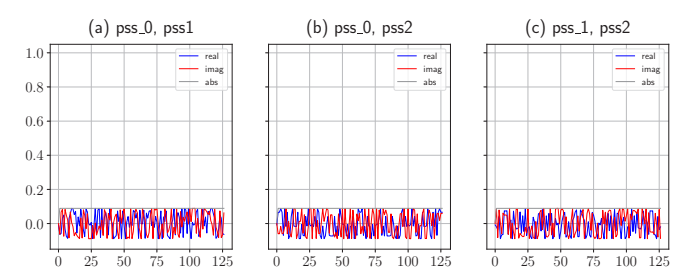


Fig. 4. Time-domain periodic cross-correlation characteristics of frequency-domain-mapped 5G NR PSS sequences.

The lengths of sequences used in the PSSs of 3GPP differ from the number of samples in a single OFDM symbol in the time domain. Frequency-domain mapping, combined with sequence conditioning (e.g., zero padding, puncturing, etc.), ensures that the resulting time-domain sequences are compatible with the OFDM frame structure. For example, in 5G NR, the PSS uses a length-127 *m*-sequence, which is significantly shorter than the 256 samples in a single OFDM symbol. Addressing this mismatch entirely in the time domain would be cumbersome and inelegant.

Theorem 1 (modulus-one sequence): Let x[0], x[1],  $\cdots$ ,  $x[N-1] \in \mathbb{C}$  and let X[k] be its N-point DFT,

$$X[k] = \sum_{n=0}^{N-1} x[n] e^{-j\frac{2\pi kn}{N}},$$
$$x[n] = \frac{1}{N} \sum_{k=0}^{N-1} X[k] e^{j\frac{2\pi kn}{N}}.$$

Define the periodic autocorrelation of X by

$$r_{XX}[\ell] = \sum_{m=0}^{N-1} X[m+\ell]X^*[m] \quad \text{(indices mod } N\text{)}.$$

The periodic autocorrelation of X is *ideal* with peak  $N^2$  (that is,  $r_{XX}[0] = N^2$  and  $r_{XX}[\ell] = 0$  for every nonzero  $\ell$ ) if and only if x has constant modulus, i.e., |x[n]| = 1 for all n.

*Proof:* We first establish the identity

$$r_{XX}[\ell] = N \cdot \text{DFT}\{|x[n]|^2\}[\ell]. \tag{3}$$

Derivation of (3). Expand  $X[m+\ell]$  and  $X^*[m]$  and sum over m:

$$r_{XX}[\ell] = \sum_{m} \left( \sum_{n} x[n] e^{-j\frac{2\pi(m+\ell)n}{N}} \right) \left( \sum_{p} x^{*}[p] e^{j\frac{2\pi mp}{N}} \right)$$

$$= \sum_{n,p} x[n] x^{*}[p] e^{-j\frac{2\pi\ell n}{N}} \sum_{m} e^{-j\frac{2\pi m(n-p)}{N}}$$

$$= \sum_{n,p} x[n] x^{*}[p] e^{-j\frac{2\pi\ell n}{N}} \delta[n-p]$$

$$= N \sum_{n} |x[n]|^{2} e^{-j\frac{2\pi\ell n}{N}}$$

$$= N \cdot \text{DFT}\{|x[n]|^{2}\}[\ell],$$

where  $\delta[n-p]$  is the Kronecker delta sequence.

 $(\Rightarrow)$  If |x[n]| = 1 for all n, then  $|x[n]|^2 = 1$ , so

$$\mathrm{DFT}\{|x[n]|^2\}[\ell] = \sum_{n=0}^{N-1} e^{-j\frac{2\pi\ell n}{N}} = N\delta[\ell].$$

By (3),  $r_{XX}[\ell]=N\cdot (N\delta[\ell])=N^2\delta[\ell],$  i.e., ideal with peak  $N^2.$ 

 $(\Leftarrow)$  If  $|r_{XX}[\ell]| = N^2 \delta[\ell]$ , take the IDFT of both sides and use (3):

$$N|x[n]|^2 = \text{IDFT}\{r_{XX}\}[n] = \frac{1}{N} \sum_{\ell=0}^{N-1} N^2 \delta[\ell] e^{j\frac{2\pi\ell n}{N}} = N.$$

Hence  $|x[n]|^2 = 1$  for all n, so |x[n]| = 1 for all n. This proves the equivalence.

Corollary 2: Let  $X[0], X[1], \dots, X[N-1] \in \mathbb{C}$  and let x[n] be its N-point IDFT,

$$x[n] = \frac{1}{N} \sum_{k=0}^{N-1} X[k] e^{j\frac{2\pi kn}{N}},$$
 
$$X[k] = \sum_{n=0}^{N-1} x[n] e^{-j\frac{2\pi kn}{N}}.$$

Define the periodic autocorrelation of x by

$$r_{xx}[m] = \sum_{n=0}^{N-1} x[n+m]x^*[n]$$
 (indices mod N).

The periodic autocorrelation of x is *ideal* with peak 1 (that is,  $r_{xx}[0] = 1$  and  $r_{xx}[m] = 0$  for every nonzero m) if and only if X has constant modulus, i.e., |X[k]| = 1 for all k.

The proof of Corollary 2 can be obtained by a minor modification of the proof of the theorem.

Note that this theorem is a special case of Wiener-Khinchin theorem, which states that the power spectral density of a wide-sense stationary random process is equal to the Fourier transform of its autocorrelation function [11].

This is a very strong result because it establishes not only that modulus-one sequences in the frequency domain produce ideal periodic autocorrelation in the time domain, but also that *only* modulus-one sequences in the frequency domain can achieve this property.

#### C. Optimality of 3GPP PSS sequences

A common misconception is that the 3GPP PSS sequences are optimized for mobile communications. This is not the case. As discussed in Section III-A and III-B, any polyphase sequence—even a random-phase sequence—can perform comparably to the current 3GPP PSS sequences in terms of correlation properties.

The 3GPP PSS sequences are derived from mathematical sequences. However, mathematical sequences are *not* designed with synchronization of radio frames in mind. They offer limited design freedom, and often result in synchronization sequences with limited performance [9]. Moreover, as discussed in Section III-A, the unique features that originally made these

mathematical sequences appealing do not always contribute to the overall performance of the resulting PSS sequences.

In contrast, Kwak et al. showed that explicitly optimizing the sequences for synchronization yields PSS sequences with substantially better correlation behavior (see Fig. 2(a) vs. Fig. 2(c) in [9]).

That said, mathematical sequences are not without merit. For example, the excellent PAPR characteristics of LTE PSS sequences stem from properties of Zadoff-Chu sequences (i.e., the DFT of a Zadoff-Chu sequence is another Zadoff-Chu sequence [12]). Interestingly, those same properties also lead to poor cross-correlation performance of LTE PSS sequences, as discussed in detail in Section III-D.

#### D. Zadoff-Chu sequences of Composite Length

Let  $x_u(n)$  be the length-N Zadoff-Chu sequence defined as

$$x_u(n) = \begin{cases} e^{-j\frac{\pi u n(n+1)}{N}}, & N: \text{ odd} \\ e^{-j\frac{\pi u n^2}{N}}, & N: \text{ even} \end{cases}$$
(4)

where  $0 \le n < N$  and 0 < u < N. If u and N share a common factor c > 1, the phase of  $x_u(n)$  becomes periodic with period  $\frac{N}{c}$  over  $0 \le n \le N-1$ , producing nonideal periodic autocorrelation with spurious peaks at nonzero lags. Thus,  $\gcd(u,N)=1$  is a necessary condition for a valid Zadoff-Chu root. Thus, Zadoff-Chu sequences of prime length are of special interest because they maximize the number of admissible roots [1].

When cross-correlations between distinct roots is important, however, root validity alone is not sufficient. The periodic cross-correlation between  $x_{u_1}(n)$  and  $x_{u_2}(n)$  contains the factor  $(u_1-u_2)$  in the exponent; if  $\gcd(|u_1-u_2|,N)>1$ , the phase again exhibits a shorter periodicity and spurious peaks appear—analogous to the autocorrelation case.

Consider the root indices  $\{25, 29, 34\}$  of Zadoff-Chu sequences of length  $63 = 3^2 \cdot 7$  (i.e., composite) used in the LTE PSS as an example. Each index is valid because it is coprime to 63. However, 34 - 25 = 9 and  $\gcd(9, 63) > 1$ , so the periodic cross-correlation between  $x_{25}(n)$  and  $x_{34}(n)$  shows spurious peaks (Fig. 5(b)). By contrast, 29 - 25 = 4 and 34 - 29 = 5 are coprime to 63, and their periodic cross-correlations do not exhibit such peaks (Fig. 5(a) and (c)).

Mapping the sequences in the frequency domain does not help in this case. The DFT of a Zadoff-Chu sequence is also a Zadoff-Chu sequence:

$$X[k] = \mathrm{DFT}\{x_u[n]\}[k] \propto x_{u'}^*[k]$$

where u' is the multiplicative inverse of u modulo 63 [12], [13]. Thus, by mapping Zadoff–Chu sequences with root indices  $\{25, 29, 34\}$  in the frequency domain, we obtain time-domain sequences that are *also Zadoff–Chu sequences*, with root indices given by the multiplicative inverses of  $\{25, 29, 34\}$  modulo 63, namely

$$(25^{-1}, 29^{-1}, 34^{-1}) \equiv (58, 34, 13) \pmod{63}.$$

The difference of 58 and 13, the multiplicative inverses of 25 and 34 modulo 63, respectively, is again *not* coprime to 63, and

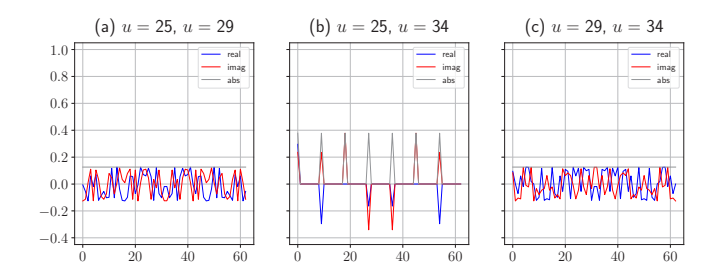


Fig. 5. Periodic cross-correlation of time-domain-mapped Zadoff-Chu sequences.  $N=63, u\in\{25,29,34\}$ . Normalized by N.

thus the periodic cross-correlation between the corresponding sequences will also generate spurious peaks (Fig. 6(b)). This is formalized in the following proposition.

Proposition 3: Let N > 1 and let a, b be integers with gcd(a, N) = gcd(b, N) = 1. Let a' and b' be the multiplicative inverses of a and b modulo N. Then,

$$\gcd(a-b,N)=\gcd(a'-b',N).$$

*Proof:* Since  $\gcd(a,N)=1$  and  $\gcd(b,N)=1$ , we have  $\gcd(ab,N)=1$ . Hence, for every  $d\mid N, d\mid ab(a'-b')$  iff  $d\mid (a'-b')$ ; therefore

$$\gcd(a'-b',N) = \gcd(ab(a'-b'),N). \tag{5}$$

Also,

$$ab(a'-b') \equiv b(aa') - a(bb') \equiv b - a \pmod{N}, \tag{6}$$

because  $aa' \equiv bb' \equiv 1 \pmod{N}$ . If two integers are congruent mod N, they differ by a multiple of N, so they have the same gcd with N. Thus, using (5) and (6), gcd(a'-b',N) = gcd(b-a,N) = gcd(a-b,N).

Why, then, choose  $\{25, 29, 34\}$  together? Because with N=63, there is no triple of valid root indices whose pairwise differences are all coprime to 63. Although there are  $\varphi(63)=36$  admissible roots (where  $\varphi(\cdot)$  is Euler's totient function), at most pairs—not triples—can satisfy the periodic cross-correlation requirement. Indeed, valid roots are coprime to  $63=3^2\cdot 7$ , so every root u satisfies  $u\equiv 1$  or  $2\pmod 3$ , where " $a\equiv b\pmod 3$ " means a and b have the same remainder when divided by 3. Take any roots  $u_1, u_2, u_3$ . By the pigeonhole principle (placing three numbers into two residue classes mod 3), at least two share the same residue modulo 3, so their difference is a multiple of 3 and thus not coprime to 63. Hence no triple can satisfy the cross-correlation requirement.

So, the better question to ask would be *Why choose length* 63? Had N been prime (e.g., N=61), any three distinct roots would be pairwise coprime in difference, yielding ideal periodic autocorrelations and cross-correlations without spurious peaks. The the additional two subcarriers obtained by using N=63 offer little performance benefit in this context.

We do not argue against using Zadoff-Chu sequences of composite length. They are suitable when the chosen configuration meets the requirements of the application and its

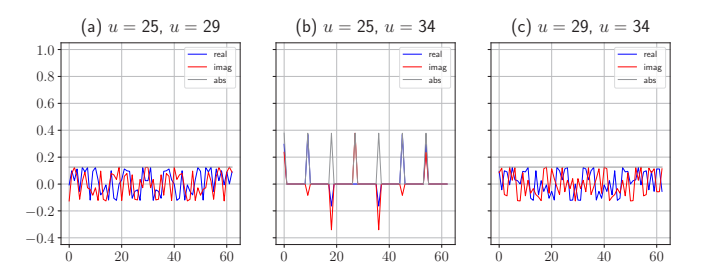


Fig. 6. Time-domain periodic cross-correlation of frequency-domain-mapped Zadoff-Chu sequences.  $N=63, u\in\{25,29,34\}.$ 

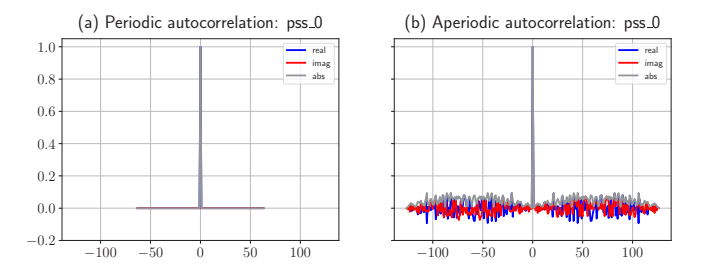


Fig. 7. Time-domain periodic and aperiodic autocorrelations of the 5G NR PSS sequence  $d_0[k]$ , mapped in the frequency domain as defined in (2). Panel (a) exhibits the *ideal* correlation because  $d_0[k]$  is a modulus-one sequence. The lags for the periodic autocorrelation in (a) range from -63 to 63, whereas those for the aperiodic autocorrelation in (b) range from -126 to 126. The two autocorrelations are identical at zero lag; however, the sidelobes of the aperiodic autocorrelation become more pronounced as |lag| increases.

operating conditions. Our point is that prime lengths generally make those requirements easier to meet—especially when multiple roots are involved—whereas composite lengths call for more careful selection and verification. When implementation constraints favor a composite length, it remains reasonable to use it, provided the design is validated against the system's performance targets.

## E. Periodic vs. aperiodic correlation

Detecting the PSS is the first step in cell search. Because the PSS has not yet been detected, the UE does not know the system timing (e.g., the OFDM-symbol boundary). Lacking this timing, the UE must use aperiodic correlation to find the PSS. Thus, PSS detection depends on aperiodic-correlation performance rather than periodic-correlation performance.

Nevertheless, we analyze periodic correlation, which is justified because periodic correlation largely reflects aperiodic behavior, especially when the lag is small (See Fig. 7). In most cases, properties observed in periodic correlation are observed in aperiodic case. When the distinction is required, we specify periodic or aperiodic; otherwise we omit the prefix.

Fig. 8 presents the *aperiodic* cross-correlation of the frequency-domain-mapped 5G NR PSS sequences, while Fig. 4 shows the corresponding *periodic* cross-correlation. Both figures exhibit the same qualitative behavior—uniformly low cross-correlation with no spurious peaks across sequence pairs. This agreement in behavior is more evident at small lags. Similarly, Fig. 6 presents the *aperiodic* cross-correlation

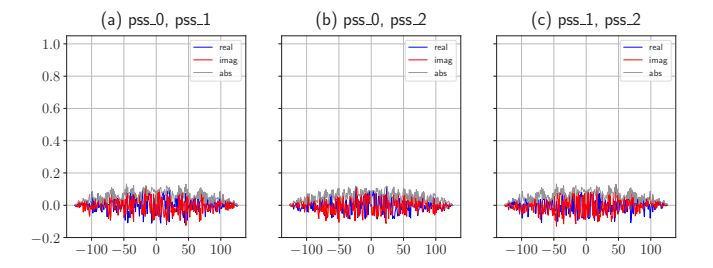


Fig. 8. Time-domain aperiodic cross-correlation characteristics of the frequency-domain mapped 5G NR PSS sequences.

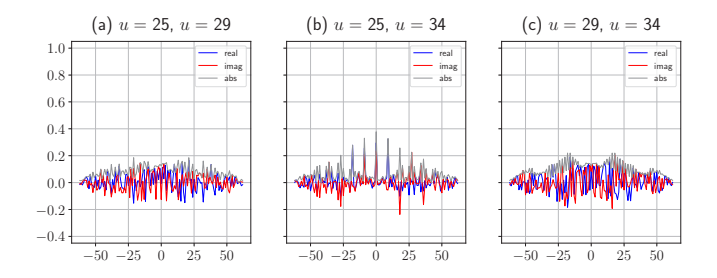


Fig. 9. Time-domain aperiodic cross-correlation characteristics of the frequency-domain mapped Zadoff-Chu sequences.

characteristics of the frequency-domain-mapped Zadoff-Chu sequences (LTE PSS), while Fig. 9 shows the corresponding *periodic* cross-correlation. Again, the spurious peaks observed in Fig. 6(b) are also observed in Fig. 9(b).

#### IV. CONCLUSION

This paper set out to dispel recurring misconceptions about the 3GPP Primary Synchronization Signals and to articulate points that are often glossed over in the literature. In this paper, we clarified where the PSS correlation properties truly come from, explained why the sequences are mapped in the frequency domain (including the role and significance of the modulus-one theorem), showed that the current PSS choices are not optimal and can be improved with optimization under the same constraints, and highlighted how sequence length affect cross-correlation behavior of Zadoff-Chu sequences.

We showed that the sharp autocorrelation peaks do not arise from special features of Zadoff-Chu or *m*-sequences themselves. They follow from using polyphase sequences together with the DFT/IDFT structure. In this view, Zadoff-Chu and *m*-sequences are just convenient instances of a broader class whose correlation properties are explained by their unit magnitude rather than by details unique to those sequence families.

We then explained why the PSS is mapped in the frequency domain. Beyond aligning naturally with an OFDM modem and simplifying resource allocation, frequency-domain mapping guarantees excellent autocorrelation peaks and generally improves cross-correlation performance. The modulus-one theorem makes this precise.

Next, we showed that today's PSS selections are effective but not optimal. With objective functions defined on the actual OFDM grid, direct optimization can yield sequences with improved correlation properties under the same practical constraints.

Finally, we emphasized that for Zadoff-Chu sequences, length and root selection matter. For composite lengths (e.g., N=63 in LTE), some root combinations can produce spurious cross-correlation peaks. We explained how these peaks arise and why, at composite lengths, avoiding them is inherently difficult.

We hope this work has achieved its aims and serves as a useful reference for understanding current PSSs and guiding synchronization sequence design in beyond-5G/6G systems.

#### REFERENCES

- Erik Dahlman, Stefan Parkvall, Johan Sköld, 5G NR: The Next Generation Wireless Access Technology, 2nd Ed., Academic Press, October 5, 2020
- [2] Hans-Jürgen Zepernick, Adolf Finger, *Pseudo Random Signal Processing: Theory and Application*, 2005, Wiley. ISBN 978-0-470-86657-3.
- [3] R. Tuninato, D. G. Riviello, R. Garello, B. Melis, and R. Fantini, "A comprehensive study on the synchronization procedure in 5G NR with 3GPP-compliant link-level simulator," in *EURASIP Journal on Wireless Communications and Networking*, vol. 2023, no. 1, p. 111, 2023.
- [4] https://www.3gpp.org/
- [5] 3GPP TS 36.211, "Evolved Universal Terrestrial Radio Access (E-UTRA); Physical Channels and Modulation", V8.9.0, 3rd Generation Partnership Project, Dec. 2009.
- [6] D. Chu, "Polyphase codes with good periodic correlation properties (Corresp.)," in *IEEE Transactions on Information Theory*, vol. 18, no. 4, pp. 531–532, July 1972.
- [7] 3GPP TS 38.211, "NR; Physical channels and modulation", v15.10.0, 3rd Generation Partnership Project, Jan. 2022.
- [8] Gilbert Strang, Linear Algebra and Its Applications, 4th Ed., Brooks/Cole, 2006.
- [9] Byung-Jae Kwak, Jin Kyeong Kim, Woncheol Cho, Young Jo Ko and Heesoo Lee, "Gradient Descent-based Optimal Sequence Design for Primary Synchronization Signal," in 2024 IEEE 100th Vehicular Technology Conference (VTC2024-Fall), Washington, DC, USA, 2024, pp. 1–6.
- [10] B. M. Popović, "Generalized chirp-like polyphase sequences with optimum correlation properties," in *IEEE Transactions on Information Theory*, vol. 38, no. 4, pp. 1406-1409, July 1992.
- [11] Steven M. Kay, Modern Spectral Estimation: Theory and Application, 1st Ed., Prentice Hall, 1988.
- [12] S. Beyme, C. Leung, "Efficient computation of DFT of Zadoff-Chu sequences," in *Electronics Letters*, vol. 45, no. 9, pp. 461–463, 2009.
- [13] David Gregoratti, Xavier Arteaga, Joaquim Broquetas, "Mathematical properties of the Zadoff-Chu sequences," arXiv preprint arXiv:2311.01035, 2023.